HHS Public Access

Author manuscript

ACS Infect Dis. Author manuscript; available in PMC 2021 March 13.

Published in final edited form as:

ACS Infect Dis. 2020 March 13; 6(3): 529–539. doi:10.1021/acsinfecdis.9b00478.

Benzothiourea Derivatives Target the Secretory Pathway of the Human Fungal Pathogen *Cryptococcus neoformans*

Sarah R. Beattie,
Department of Pediatrics, Carver College of Medicine, University of Iowa, Iowa City, Iowa 52245, United States

Nicholas J. Schnicker,
Protein and Crystallography Facility, Carver College of Medicine, University of Iowa, Iowa City, Iowa 52245, United States

Thomas Murante,
Department of Pediatrics, University of Rochester, Rochester, New York 14642, United States

Kavitha Kettimuthu,
Department of Biochemistry, University of Texas Southwestern, Dallas, Texas 75390, United States

Noelle S. Williams,
Department of Biochemistry, University of Texas Southwestern, Dallas, Texas 75390, United States

Lokesh Gakhar,
Protein and Crystallography Facility, Carver College of Medicine and Department of Biochemistry, Carver College of Medicine, University of Iowa, Iowa City, Iowa 52245, United States

Damian J. Krysan
Department of Microbiology and Immunology, Carver College of Medicine and Department of Pediatrics, Carver College of Medicine, University of Iowa, Iowa City, Iowa 52245, United States

Abstract

Cryptococcus neoformans is one of the most important human fungal pathogens and causes life-threatening meningoencephalitis in immunocompromised patients. The current gold standard

Corresponding Author: Damian J. Krysan – *Department of Microbiology and Immunology, Carver College of Medicine and Department of Pediatrics, Carver College of Medicine, University of Iowa, Iowa City, Iowa 52245, United States*; Phone: 319-335-3066; damian-krysan@uiowa.edu.

Author Contributions

S.R.B., N.S., L.G., N.S.W., and D.J.K. designed the experiments. S.R.B., T.M., N.S., and K.K. performed the experiments. The manuscript was written by S.R.B. and D.J.K.

Notes

The authors declare no competing financial interest.

Supporting Information

The Supporting Information is available free of charge at https://pubs.acs.org/doi/10.1021/acsinfecdis.9b00478.

Table S1: fractional inhibitory concentration indices (FICI) of **1** with clinical antifungals. Figure S1: BTU treatment induces a cell separation defect. Figure S2: BTU derivatives do not affect Rho1 GTP hydrolysis. Figure S3: intrinsic GTPase activity or GDP/GTP exchange is not affected by BTU derivatives (PDF)

therapy for *C. neoformans* meningoencephalitis is based on medications that are over 50 years old and is not readily available in regions with high disease burden. Here, we report the mycologic, mechanistic, and pharmacologic characterization of a set of benzothioureas with highly selective fungicidal activity against *C. neoformans*. In addition, to direct antifungal activity, benzothioureas inhibit *C. neoformans* virulence traits. On the basis of a set of phenotypic, biochemical, and biophysical assays, the benzothioureas (BTUs) inhibit the late secretory pathway (post-Golgi), possibly through a direct interaction with Sav1, an orthologue of the Sec4-class small GTPase. Importantly, pharmacological characterization of the BTUs indicates it readily penetrates the blood-brain barrier. Together, our data support the further development of this scaffold as an antifungal agent with a novel mechanism of action against *C. neoformans*.

Graphical Abstract

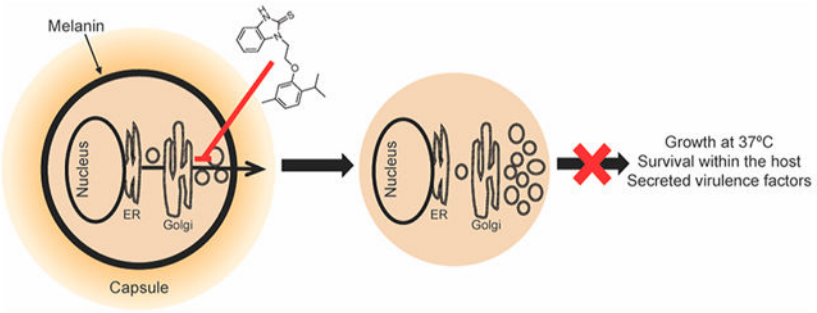

Keywords

Cryptococcus; antifungal; secretory pathway; fungicidal; blood-brain barrier

Cryptococcus neoformans is the most common cause of meningitis in HIV/AIDS patients and a significant cause of morbidity and mortality among immune-compromised patients worldwide.[1,2] Despite available therapies, mortality rates remain high, reaching up to 70% in resource-limited regions and 20–40% in Europe and the United States.[2] A critical aspect of treatment outcomes is early fungicidal activity. Studies comparing the survival rate to organism clearance show that fungicidal drugs that more rapidly reduce fungal burden in cerebrospinal fluid (CSF) are associated with better outcomes than fungistatic drugs or less rapid sterilization.[3–5] Therefore, our efforts have been focused on the identification and development of candidate anti-cryptococcal molecules with fungicidal activity.

Previously, we identified *N*-substituted benzothioureas (BTU; Figure 1) as a novel anti-cryptococcal scaffold from a high-throughput screen designed to identify molecules that target cell-wall-related processes.[6] BTUs inhibit the growth of *C. neoformans* with varying potency, and the IC_{50} increases by at least 1.5-fold in the presence of sorbitol, indicating that cell death is due, in part, to cell-wall destabilization.[6] Further supporting cell-wall disruption as their general mode of action, BTU derivatives inhibit the activation of the cell-wall integrity pathway (CWIP) in response to the cell-wall perturbing agent, calcofluor white.[6] Specifically, BTUs reduced the activation of the CWIP-regulated transcription factor Rlm1 and decreased the phosphorylation of the CWIP MAP kinase, Mpk1, during cell-wall stress.

BTUs do not, however, directly inhibit protein kinase C (PKC),[6] an essential kinase that acts upstream of the CWIP.[7] While the effect of BTU derivatives on the cell wall is apparent, their molecular target and mechanism of action are still unclear.

To further characterize the mechanism of action of the BTU scaffold, we assessed its effect on several cellular phenotypes and found that it inhibits secretory pathway function as its primary mode of action. This pathway is required for many essential processes in fungi, and thus, many key components are essential for viability.[8–10] The secretory pathway has been extensively studied in *Saccharomyces cerevisiae* and is a multistage process governing the trafficking of proteins from the ER to Golgi to plasma membrane or to other membrane-bound organelles, such as vacuoles or multivesicular bodies (reviewed in reference 11).

Cargo destined for exocytosis is transported from the Golgi to the plasma membrane in secretory vesicles, which dock and fuse with the membrane *via* the interaction of the Rab family GTPse, Sec4, and the exocyst,[12,13] a complex of eight proteins that assembles on the plasma membrane.[14] In contrast to other small GTPases, such as Ras, the function of Sec4 is dependent on the ability to cycle between GTP- and GDP-bound states, not only the amount of total active Sec4 in the cell.[15,16] GTP-bound Sec4 is loaded onto secretory vesicles, and then, the hydrolysis of GTP is coupled with the release from the vesicle membrane following exocytosis.[15,17]

In *C. neoformans*, the secretory pathway is essential for the production of virulence factors, most of which are located at the cell periphery or in the extracellular space.[18–20] The Sec4 homologue in *C. neoformans* is called Sav1 (secretion-defect and accumulated vesicle), not Sec4, due to the inability of this protein to complement the Sec4 temperature-sensitive mutants in *S. cerevisiae*.[19] Like its *S. cerevisiae* counterpart, Sav1 is essential and temperature sensitive ($sav1^{ts}$) mutants display a reduced secretion of acid phosphatase, impaired trafficking of the capsule polysaccharide, glucuronoxylomannan (GXM),[19] and aberrant intracellular membrane structures.[21] Two additional secretory components have been studied in *C. neoformans*: the exocyst complex protein, Sec6[20], and the phosphatidylinositol transport proteins, Sec14–1 and Sec14–2.[18] These studies highlight the distinct secretory routes for different virulence factors and only scratch the surface of the complexity and importance of intracellular transport in a pathogenic yeast.

Here, we characterize the most potent of the BTU molecules, **1**. We show that this molecule inhibits melanin synthesis and capsule production in *C. neoformans*. Furthermore, we identify the mode of action of **1** as inhibition of the secretory pathway and provide biophysical evidence that it interacts with the Sec4-like GTPase Sav1. Finally, **1** readily penetrates the blood-brain barrier (BBB), making this scaffold attractive for development as anti-cryptococcal meningitis drugs.

RESULTS

BTU Derivatives Are Fungicidal against *C. neoformans*.

BTU derivatives were identified in a screen for molecules that were fungicidal against *C. neoformans* H99 and showed evidence of interfering with the cell-wall integrity pathway. To

further evaluate the antifungal spectrum of activity for the BTUs, we tested the minimum inhibitory concentration (MIC) of **1** against a panel of *C. neoformans* clinical isolates, references strains, and other species of human fungal pathogen. The MIC for all tested *C. neoformans* strains was 2–4 μg/mL, regardless of the susceptibility to other antifungals (Table 1). Despite potent anti-cryptococcal activity, **1** was not active against the ascomycete pathogens *Candida albicans*, *Aspergillus fumigatus*, and *Fusarium oxysporum* or the model organism *S. cerevisiae.* Interestingly, **1** had activity against the zygomycete *Mucor circinelloides* with an MIC of 8 μg/mL (Table 1).

To determine the killing kinetics and minimal fungicidal concentration (MFC) of **1** against *C. neoformans*, we performed time-kill experiments. Treatment with 4 μg/mL was fungistatic over 30 h of treatment, whereas **1** was fungicidal at 8 and 16 μg/mL (~2 $\log_{10}$ reduction in CFU relative to the starting inoculum), respectively, after 24 h of treatment (Figure 2A). We did not observe synergy with 5-flucytosine, amphotericin B, or fluconazole against *C. neoformans* (Table S1). In addition to **1**, we also determined the MIC of five analogues against *C. neoformans* reference strain H99. The analogues showed varying degrees of antifungal activity, with compound **3** lacking antifungal activity at the highest achievable concentration in solution (Figure 1). The *in vitro* activity of **1** toward *C. neoformans* makes this drug an attractive candidate for antifungal development.

BTU Modulates the Expression of *C. neoformans* Virulence Traits.

C. neoformans has an arsenal of virulence factors that contribute to its pathogenicity and/or ability to survive within the host. One such trait is the ability to replicate in the phagolysome of macrophages.[22] It is thought that intracellular yeast can disseminate throughout the body using a “Trojan horse” mechanism to cross the BBB to establish an infection in the CNS.[23] To measure the drug activity against intracellular *C. neoformans*, we exposed the murine macrophage-like J774 cells to *C. neoformans*, removed the extracellular yeast, and treated the co-cultures with **1**. After 24 h, the intracellular burden of J774 cells was significantly reduced by 82 (±5)% with 4 μg/mL **1** and 91 (±3)% with 8 μg/mL **1** as compared to controls (Figure 2B). These results indicate that **1** has activity against *C. neoformans* within a key host niche. It is important to note that neither fluconazole nor amphotericin B have fungicidal activity against intraphagocytic *C. neoformans*.[24]

A unique virulence factor of *C. neoformans* compared to other human fungal pathogens is the production of a polysaccharide capsule. The capsule has a critical role in survival within the host and is required for virulence.[25] Treatment with **1** (2 μg/mL) reduced the capsule formation under two conditions that induce capsule formation: physiological CO_2 (DMEM, 5% CO_2) and nutrient limitation (10% Sabouraud dextrose broth [10% Sab], pH 8). Under both conditions, untreated controls produced thick capsules, while drug-treated cells had a reduced capsule size, with some cells producing little to no capsules (Figure 3A).

C. neoformans also generates melanin, a polyaromatic pigment ultimately produced by the diphenol oxidase, laccase.[26,27] Melanin is hypothesized to protect against immune defenses such as the oxidative burst, phagocytosis, and antimicrobial peptides.[28] Treatment with a sub-inhibitory concentration of **1** inhibited melanization on solid media containing L-DOPA

(Figure 3C). Overexpression of one of the laccase isoforms, *LAC1*, did not overcome the inhibition of melanization by **1**, indicating it was unlikely to directly inhibit Lac1; consistent with that notion, we observed no effect of **1** on the laccase activity of cellular lysates (data not shown). We utilized a strain bearing a GFP-tagged Lac1 to assess the effect of **1** on its localization. Lac1 localizes to the cell periphery (Figure 3B) and associates with the cell wall, as previously reported.[29,30] Treatment with **1** led to an accumulation of Lac1-GFP in the cytoplasm (Figure 3B), indicating it affects either the trafficking or incorporation of Lac1-GFP into the cell wall. These data indicate that **1** interferes with two of the most important *C. neoformans* virulence factors: melanization and capsule formation. A recent analysis of patient outcome data has shown that strains with reduced ability to express these two virulence traits are associated with improved organism clearance and survival.[31]

BTU Derivatives Inhibit the Secretory Pathway As the Mode of Action.

Trafficking of laccase to the cell periphery is dependent on the secretory pathway and the exocyst complex protein, Sec6.[20] Similarly, capsule trafficking is at least partially dependent on exocytosis through the secretory pathway and the GTPase, Sav1.[19] Therefore, we hypothesized that the effect of **1** on the virulence factors in *C. neoformans* is due to the inhibition of the secretory pathway. To test this hypothesis further, we examined the effect of **1** on secretion of acid phosphatase to the cell surface. Acid phosphatase secretion is dependent on the secretory pathway in *S. cerevisiae*[8,32] and has been similarly shown to be dependent on the Sec4 orthologue, Sav1, in *C. neoformans*.[19] Treatment of *C. neoformans* with **1** for 6 h inhibited secretion in a dose-dependent manner with an observed IC_{50} of 0.84 (±0.3) μg/mL (Figure 4A). To ensure that the observed decrease in secretion is not a result of cell death, we stained cells that had been exposed to 0, 1, and 4 μg/mL of **1** with propidium iodide to determine the proportion of live versus dead cells. At 1 μg/mL of **1**, just above the acid phosphatase secretion IC_{50}, ~4% of cells stained positively with PI, compared to 1.5% in the control (Figure 4B). Importantly, the inactive BTU, 3, does not inhibit acid phosphatase secretion at the highest achievable concentration, even after 18 h of incubation (Figure 4D). Under these conditions, the IC_{50} of **1** is 1.94 (±0.40) μg/mL (Figure 4C). Together, these data strongly support the hypothesis that BTU derivatives inhibit the secretory pathway as part of their mode of antifungal activity.

Inhibition of the secretory pathway in *S. cerevisiae* manifests different phenotypes based on where the block occurs in the pathway. Early secretory pathway (ER to Golgi) mutants accumulate ER membrane or small vesicles (<80 nm), whereas mutants affecting the late secretory pathway (Golgi to plasma membrane) accumulate vesicles 100–200 nm in size.[10] Transmission electron microscopy (TEM) of *C. neoformans* cells treated with 1 under nutrient limiting, capsule-inducing conditions showed the accumulation of membrane vesicles (Figure 5). These vesicles range in size but are generally larger (>80 nm), suggesting they are post-Golgi vesicles. These data strongly support the idea that BTUs block the secretory pathway and suggest that this block occurs in the late secretory pathway.

Consistent with the previously characterized effect of BTU compounds on the cell wall and the inhibition of the activation of the cell-wall-integrity pathway,[6] we also observed defects in the cell wall by TEM (Figure 5). Rather than having a cell wall of uniform thickness, the

cell wall in cells treated with **1** is irregular and, in many cases, the outer dense layer is thin and incompletely surrounds the cell body (Figure 5). We also observed a cell-separation defect, where an apparent septum is formed, but the daughter cells remain attached to the mother cell. BTU-treated cells show a 2-fold higher percentage of cells with 3, 4, or ≥5 cell bodies (one cell body defined by invagination between two rounded compartments) compared to control cells (Figure S1). Cell separation defects have also been observed in the *sav1*^{ts} mutant in *C. neoformans*.[19] Collectively, these data further indicate that BTU derivatives disrupt the secretory pathway function.

BTU Derivatives Interact with the *C. neoformans* Sec4 Orthologue, Sav1.

The cell-wall integrity and the secretory pathways are both regulated by the Rho GTPase, Rho1.[33] Accordingly, we hypothesized that Rho1 would be a reasonable candidate target for BTU derivatives. We, therefore, tested the effect of **1** on *Cn*Rho1 GTPase activity. To do so, we expressed recombinant *Cn*Rho1 (CNAG_03315) in *Escherichia coli* and purified it using affinity chromatography. *Cn*Rho1 hydrolyzed GTP as expected, and treatment with 25 μg/mL **1** did not affect its enzymatic activity over 80 min of incubation (Figure S2). Although it is possible that **1** could affect other aspects of *Cn*Rho1 function such as binding partner interaction or localization, we explored other potential targets.

Cell-wall integrity depends on the secretory pathway for transport of synthetic enzymes, cell-wall material, and cell-wall- and membrane-associated proteins. Moreover, the inhibition of secretion blocks the transport of essential signaling molecules, such as Rho1, to the cell surface after synthesis.[34] Therefore, we hypothesized the block in secretion may be a result of the direct inhibition of a secretory component. Sav1 is an essential protein of the late (post-Golgi) secretory pathway, and the temperature-sensitive mutant produces phenotypes similar to **1** treatment; therefore, we hypothesized Sav1 to be the target of **1**. Furthermore, this is supported by the circumstantial evidence that Sav1 cannot complement *sec4*,[19] Sec4 homologues are not essential in *A. fumigatus*,[35] and **1** is not active against these organisms.

Sec4-class GTPases cycle between the Golgi apparatus and the plasma membrane. We, therefore, obtained a strain bearing a fluorescently tagged version of Sav1 (DsRed-Sav1). As previously reported, Sav1 localizes most often as a single punctum within the cell (Figure 6A). However, BTU exposure results in a diffuse signal throughout the cell (Figure 6A and B). Indeed, vesicular structures and aggregates with a DsRed-Sav1 signal are readily apparent within many cells (Figure 6B). These data are consistent with previous data indicating that **1** inhibits the secretory pathway and results in post-Golgi vesicle accumulation within the cell. Still, these data do not discriminate whether BTU is directly or indirectly affecting the localization of Sav1.

To determine if the cellular effect of **1** on Sav1 localization may be direct, we tested whether BTUs interact with Sav1. We expressed and purified recombinant Sav1 (CNAG_02817) in *E. coli*. Like its *S. cerevisiae* orthologue, recombinant Sav1 showed low but measurable intrinsic GTPase activity (Figure S3A) and underwent GDP-GTP exchange reactions (Figure S3B). Sec4-related GTPases also bind to GDP as part of their recycling between the plasma membrane and the late Golgi. To confirm that the recombinant Sav1 was able to bind GDP,

we used a thermal-shift assay to measure the effect of GDP on thermal denaturation of the protein. Consistent with expectations, recombinant Sav1 was stabilized by both GDP and GTP (Figure 6C). The function of Sec4-like proteins not only is dependent on their enzymatic activity but also requires it to bind to both proteins and membranes. Since these other functions are difficult to assess, we instead asked if **1** interacts with Sav1 using the same thermal-shift assay. As shown in Figure 6D, **1** (20 μM) lowered the T_m of Sav1 by ~4 °C, an effect consistent with it directly interacting with Sav1. The destabilizing effect of **1** on Sav1 was abrogated by the presence of GDP (50 μM), indicating that the molecule is unlikely to directly denature Sav1. Importantly, the interaction of Sav1 with **1** showed a smooth dose response (Figure 6E). Furthermore, the structurally similar, inactive benzothiourea **3** had no effect on Sav1 T_m up to the limit of solubility (Figure 6F), while an analogue with intermediate antifungal and antisecretory pathway activity, **2** (MIC = 8 μg/mL; Figure 1), showed correspondingly intermediate interaction with Sav1. These biophysical data show that the interaction of BTUs with Sav1 correlates with antifungal activity and are consistent with the possibility that BTUs may directly interact with Sav1 a part of their antifungal activity.

Next, to determine if **1** could modulate Sav1 activity, we measured the intrinsic rate of GTP hydrolysis in the presence and absence of **1**. Sav1 intrinsic GTPase activity was, however, not affected by concentrations of **1** up to 25-fold higher than MIC (Figure S3A). In addition, we did not observe any effect of **1** on the intrinsic GDP/GTP exchange rate (Figure S3B) nor on the apparent rate of GDP exchange (data not shown). It is important to consider that Sec4 class proteins function with GTPase activating proteins, GDP exchange factors, and within multiprotein complexes. As such, there are other possible interactions that may be disrupted by BTUs binding to Sav1.

BTU Penetrates the Blood-Brain Barrier.

A challenging aspect of developing drugs to treat CNS infections is the capriciousness of BBB drug penetration. Given the specificity of the BTUs against *Cryptococcus*, we tested its ability to cross the BBB in order to determine whether this class of drug has potential for use in the treatment of cryptococcal meningitis. First, we determined the tolerability of BTU and found that the maximum tolerated dose of **1** was 50 mg/kg through a set of dose escalation experiments. Second, we determined whether BTU could penetrate the brain and what concentrations were established at that dose. Previous experiments had shown the molecule was stable in serum.[6] Single dose (50 mg/kg) pharmacokinetics showed that **1** penetrates the BBB and achieves a maximum concentration (C_{max}) of 1.80 μg/mL in the brain tissue and 2.01 μg/mL in the serum (Figure 7A). This indicates that a significant portion of the plasma drug penetrates the CNS (AUC_{Brain}/AUC_{Serum} ratio of 1.6). Importantly, the $T_{1/2}$ values for **1** are quite robust with the serum and brain values being 240 and 184 min, respectively (Figure 7B).

To test the efficacy of **1** *in vivo*, we used the well-established murine model of disseminated cryptococcosis.[36] In this model, *C. neoformans* is directly inoculated into the bloodstream *via* the tail vein, which allows for rapid establishment of infection in the brain. Mice inoculated with H99 were treated with **1** (50 mg/kg) 3 times daily for 2 days. Enumeration

of colony forming units of brain homogenates showed no significant reduction in burden between **1**-treated mice and controls (Figure 7C). This lack of efficacy is likely due to the fact that the maximum serum and brain tissue concentrations are nearly equal to MIC. Typically, anti-infectives need to achieve concentrations above MIC directly or accumulate to such levels. Despite this lack of *in vivo* efficacy, the pharmacological properties of this drug make it a promising candidate for medicinal chemistry-based optimization of its anti-cryptococcal activity.

DISCUSSION

Here we report the characterization of a novel anti-cryptococcal scaffold, the BTUs. Our data indicate that BTUs inhibit the secretory pathway as part of the mode of action, potentially through a direct interaction with the Sec4 class GTPase, Sav1. Although the intrinsic GTPase activity of Sav1 was not altered by **1** treatment, there are many possibilities as to how binding of **1** to Sav1 could alter function. In this study, we measured the intrinsic activity of Sav1 *in vitro.* However, GTP hydrolysis is very slow without the interaction of a GTPase activating proteins (GAPs), which enhance the rate of hydrolysis, and guanine nucleotide exchange factors (GEF), which facilitate the release of GDP, allowing GTP to bind and reset the GTPase to its active form.[37–39]

One possibility is that the binding of **1** to Sav1 interferes with GAP or GEF interactions, dampening or inhibiting the effects of these rate-enhancing partners. Additionally, the function of Sec4 is more complex than other small GTPases, and depends on not only the nucleotide binding state but also the localization within the cell. It is also possible that BTU disrupts the binding interactions between partners that correctly localize Sav1 to the secretory vesicle membrane, the plasma membrane, or the cytosol, preventing the cycling on and off vesicles that are required for function. Finally, BTU might inhibit the interaction with effector proteins, such as the exocyst complex protein Sec15, which directly binds ScSec4, to target vesicles to sites of exocytosis at the plasma membrane.[12]

Although the ability of a molecule to stabilize proteins is most commonly taken to be evidence of binding interactions in the context of thermal-shift assays, molecules that induce protein destabilization can also be important interactors. One mechanism for this interaction is that the molecule binds to and stabilizes a partially or completely unfolded state of the protein.[40] A less extreme version of this model is that a protein may have a variety of conformations that are in equilibrium and that the molecule interacts with an energetically less favored, but not inaccessible, conformation. In the case of Sec4-class GTPases, they adopt a variety of conformations depending on whether GDP or GTP are bound;[17] indeed, in the absence of bound guanine nucleotide, the proteins are unstable. However, at this time, we have not been able to either crystallize a protein-drug complex nor have we experimentally identified the consequences of the putative interaction of BTUs with Sav1. Thus, we can conclude that the BTUs interfere with the secretory pathway in *C. neoformans*, but we cannot definitively conclude that Sav1 is the molecular target.

The secretory pathway is critical for the expression of *C. neoformans* virulence factors. Inhibition of this pathway prevents surface localization of melanin and capsule

polysaccharides, both of which are crucial for protection against phagocytosis.[29,41–43] The reduced ability to produce these virulence factors is associated with better patient outcomes[31] and *in vitro*, melanized Cryptococcal cells are more resistant to amphotericin B treatment.[44] Thus, the ability to modulate these virulence factors *in vivo* has the potential to improve patient outcomes while also boosting efficacy of other antifungal drugs. Therefore, future studies with BTUs could also explore the use of these compounds as adjuvants to existing therapies. Additionally, the ability to kill *C. neoformans* within macrophages not only is significant in reducing the burden within a key host niche but also has potential in reducing dissemination to the brain. We hypothesize that BTU treatment would reduce the number of cells that cross the BBB by the "Trojan horse" mechanism through the killing of intracellular yeast. Our previous studies also showed that BTUs are more active at 37 °C.[6] Together, the ability to inhibit critical virulence factors is a unique feature of the BTU derivatives.

Another extremely favorable feature of BTUs is their pharmacological properties. While initial *in vivo* studies did not show a reduction in brain burden, the levels in the serum reach 2 μg/mL, just at the level of MIC, and do not maintain concentrations at or above MIC for very long. Typically, C_{max} or AUC in serum or tissue needs to be well over MIC or the serum/tissue concentration needs to maintain a concentration over MIC for a prolonged period of time for molecules to have in vivo efficacy.[45] However, the ability to readily penetrate the BBB and enter the brain tissue is a very desirable characteristic. The majority of small molecules (98%) do not cross the BBB.[46] Thus, a compound with anti-cryptococcal activity that already has favorable neurological pharmacokinetics is a great advantage at the start of an optimization campaign. Medicinal chemistry to improve the potency of the molecule is a promising avenue for development of a cryptococcal meningitis treatment. In summary, this work characterized a novel antifungal scaffold with a new mode of action and very promising pharmacological properties. Furthermore, these studies highlight the potential of the secretory as an antifungal drug target, which can be exploited for future identification of novel antifungal drugs.

METHODS

Strains, Media, and Chemicals.

C. neoformans clinical isolates (DUMC series) were provided by Dr. John Perfect, Duke University Medical Center. *A. fumigatus* and *Fusarium* strains were provided by Dr. Robert Cramer, Dartmouth College. *M. circinelloides* strains were provided by Dr. Joseph Heitman, Duke University. The Lac1-GFP strain was provided by Dr. John Panepinto, University at Buffalo. The DsRed-Sav1 was provided by Dr. Ping Wang, Louisiana State University Health Sciences Center, New Orleans. *C. neoformans* strains were maintained on YPD and stored at −80 °C in 25% glycerol. For all experiments, cells were enumerated by hemocytometer. All BTU compounds were obtained from ChemBridge: **1** = ChemBridge ID #7794378, **2** = ID #5673353, **3** = ID #6571801, **4** = ID #5672032, **5** = ID #6762995, and **6** = ID #5682634. The synthesis of BTU has been previously described;[6] however, compounds in this study were purchased from ChemBridge. The purity of compound 1 is 95%, as measured by CG-MS.

Minimum Inhibitory Concentration and Fractional Inhibitory Concentration Index Determination.

Minimum inhibitory concentrations were determined using CLSI guidelines.[47,48] All yeasts were cultured overnight in 3 mL of YPD at 30 °C and then washed twice in sterile PBS. Then, 2-fold serial dilutions of each drug were prepared in RMPI+MOPS pH 7 (Gibco RPMI 1640 with L-glutamine [11875–093] and 0.165 M MOPS), and then, 1×10^3 cells were added per well. Plates were incubated at 37 °C for 24 (*C. albicans* and *S. cerevisiae*) or 72 (*C. neoformans*) h. For *A. fumgiatus*, *F. oxysporum*, and *M. circinelloides*, the wells were inoculated with 1.25×10^3 conidia. Plates were incubated at 37 °C for 48 h for *A. fumigatus* and *M. circinelloides* and 72 h for *F. oxysporum*. For fractional inhibitory concentrations, we performed standard checkerboard dilution assays.[49] Then, 1×10^3 cells of H99 were added, and the plates were incubated for 72 h; then, the MIC was determined for each drug alone and each drug in combination. The fractional inhibitory concentration index was determined by the following expression: $(MIC_{A,alone}/MIC_{A,combo}) + (MIC_{B,alone}/MIC_{B,combo})$. Each assay was done in technical duplicates, and at least two independent experiments were performed on different days.

Time-Kill Assay of BTUs.

An H99 overnight culture was washed and diluted to 10^5 cells/ml in RPMI+MOPS pH7 with DMSO or 4, 8, or 16 μg/mL **1**. Then, 200 μL of cells was dispensed into a 96 well-plate, and the plate was incubated at 37 °C for 30 h. At each time point, a single well was resuspended and diluted in a 10-fold series in PBS and plated on YPD. Each experiment was performed in triplicate and plated in technical duplicate. These data are representative of two independent experiments performed on separate days.

Antifungal Activity of BTUs against Intraphagocytic *C. neoformans*.

The murine macrophage-like J774 cells (1×10^5) were seeded in 24-well plates and incubated overnight at 37 °C, 5% CO_2. *C. neoformans* H99 was cultured overnight, washed three times in sterile PBS, and then diluted to 5×10^5 CFU/ml with 2 μg/mL anti-*Cryptococcus* antibody 18b7 (gift from Dr. Arturo Casadevall). Cells were incubated for 1 h at 37 °C with rotation, and then, 100 μL of the cell suspension was added to each well of J774 cells and incubated for 1 h and 20 min at 37 °C. The medium was removed, and the wells were gently washed with sterile PBS to remove unengulfed cells. Fresh media with DMSO, 4 μg/mL or 8 μg/mL 1, was added to the cells, and the plates were incubated at 37 °C, 5% CO_2 for 24 h. J774 cells were lysed in 600 μL of ice-cold 0.2% Triton-X for 10 min, and then, 10-fold serial dilutions of lysate were plated on YPD. Each experiment was performed in triplicate and plated in technical duplicate. These data are representative of two independent experiments performed on separate days.

C. neoformans Melanization Assay.

C. neoformans H99 was cultured overnight in YPD at 30 °C, washed twice in sterile PBS, and then diluted to 1×10^6 CFU/ml in sterile PBS. Cells were spotted on defined asparagine minimal media (7.6 mM L-asparagine, 5.6 mM glucose, 22 mM KH_2PO_4, 1 mM $MgSO_4$-$7H_20$, 0.3 mM thiamine-HCl, and 20 nM biotin) with 0.5 mM L-DOPA (3,4-

dihydroxy-L-phenylalanine; Sigma) with DMSO or 8 μg/mL **1**. The plates were incubated at 37 °C, and the development of melanin pigment was monitored over 3 days.

For laccase-localization studies, a strain bearing Lac1-GFP was spotted at 37 °C on asparagine minimal media containing 1 mM L-DOPA with DMSO or 2 μg/mL **1**. Colonies were picked from each plate and resuspended in sterile water, and then, GFP was imaged with a Nikon epifluorescence microscope with a Cool Snap HQ2 camera and Nikon Elements image acquisition and analysis software. Assays were performed in triplicate at least twice on independent days.

C. neoformans Capsule Formation Assay.

C. neoformans H99 was cultured overnight in YPD at 30 °C, and then, the cells were washed twice in sterile PBS and diluted to 1×10^6 CFU/ml in Dulbecco's Modified Eagle medium (DMEM; Gibco 11965–092) or 10% Sabouraud dextrose broth pH 8. DMSO or indicated concentrations of drug was added to cells, and then cells were dispensed into 24-well plates and incubated at 37 °C for 24 (10% Sab) or 48 h (DMEM, with 5% CO_2). Cells were washed in PBS, then mixed in a 1:1 ratio with India ink (Becton, Dickinson and Company) on a microscope slide. Brightfield images were acquired on a Nikon epifluorescence microscope with a Cool Snap HQ2 camera and Nikon Elements image acquisition and analysis software. For cell separation quantification, cells grown under 10% Sab conditions for 24 h with 1 μg/mL **1** were washed in PBS, and then brightfield images were acquired. Cell bodies were defined rounded cellular compartments separated by invaginations. At least 150 cells were counted per sample of triplicates.

Acid Phosphatase Secretion Assay.

Acid phosphatase secretion was measured on intact cells as previously described[19] with the follow modifications. *C. neoformans* H99 was cultured overnight in 25 mL YNB media supplemented with 0.5% KH_2PO_4 at 30 °C. Cells were washed three times with YNB media without phosphate (supplemented with 0.5% KCl), and then, cells were diluted to 1×10^7 CFU/mL in YNB without phosphate +0.5% KCl. DMSO or indicated drugs were added in a 2-fold dilution series, and then, 3 mL of cell suspension was dispensed into 6-well plates and plates were incubated at 37 °C for 18 h. One mL of each culture was harvested and resuspended in 400 μL of 2.5 mM paranitophenylphosphate (p-NPP, Sigma; in 50 mM acetate buffer, pH 4) and the reaction was incubated at 37 °C for 5 min. Each reaction was stopped with 800 μL of saturated Na_2CO_3, and A_{420} was read by spectrophotometer. A_{420} readings were normalized to cell density (A_{600}). These data are represented as the percent of the control (DMSO) and represent technical triplicate. At least two independent assays were performed for each drug on different days. Aliquots from indicated concentrations were washed in PBS, then resuspended in PBS with 5 μg/mL propidium iodide (Invitrogen). Samples were imaged in bright field (total cell number) and red channels using a Nikon epifluorescence microscope with a Cool Snap HQ2 camera and Nikon Elements image acquisition and analysis software. At least 100 cells from each replicate were counted.

Rho1 Purification and GTPase Activity Assay.

A plasmid bearing 6XHis-*Cn*Rho1 (CNAG_03315) was transformed into One Shot BL21 (DE3) *E. coli* cells (Invitrogen). A single colony was inoculated into LB + Ampicillin and grown overnight at 37 °C and then subcultured in 250 mL LB + Ampicillin for 3 h at 30 °C. Then, 50 mL of the culture was collected for the uninduced fraction, and then, the culture was induced with 0.5 mM isopropylthio-β-galactoside (IPTG; Invitrogen) and continued incubation for 1 h. Cell pellets were lysed in Qiagen native lysis buffer with benzonase, lysates were applied to the Ni-NTA column (Ni-NTA Fast Start Kit, Qiagen), and purification was performed following the manufacturers' instructions. Protein was eluted with two rounds of 750 μL of elution buffer. Each fraction was run on an SDS-PAGE gel. Rho GTPase activity was measured using the GTPase-Glo (Promega) Assay kit. Then, 800 ng of Rho1 per reaction was preincubated with 25 μg/mL 1 or DMSO for 30 min at room temperature (RT), and then, the GTPase reaction was started with 1 μM GTP and 1 mM DTT per the manufacturers' instructions. The reactions were stopped at indicated time points and developed per manufacturers' instructions. The luminescence was read with a 100 ms integration time.

Sav1 Protein Expression and Purification.

SAV1 (CNAG_02817) from *C. neoformans* was overexpressed in *E. coli* BL21 (DE3) cells with an N-terminal 6 Histidine tag using the pET15b expression vector. The cells were grown in LB media at 37 °C until reaching an optical density of ~0.5 at 600 nm, and then, they were lowered to 18 °C, induced with 0.5 mM IPTG, and harvested after overnight growth. The cells were resuspended in lysis buffer (50 mM HEPES pH 8.0, 500 mM NaCl, 10 mM imidazole, 1 mM TCEP, 5% glycerol) with an EDTA-free protease tablet (Roche), lysozyme, and DNase and were lysed by sonication. The soluble fraction was loaded onto a 5 mL Ni-NTA agarose column (Qiagen) equilibrated in lysis buffer. The nonspecifically bound proteins were washed away with 10 column values of lysis buffer containing 30 mM imidazole. A linear gradient (50 mL) was used to elute Sav1 with lysis buffer containing 500 mM imidazole. Protein purity was assessed by SDS-PAGE, and fractions of >95% purity were pooled and concentrated to load onto a Superdex 200 16/60 column (GE Healthcare) equilibrated in SEC buffer (50 mM HEPES pH 8.0, 150 mM NaCl, 1 mM THP, 5% glycerol). The fractions were again assessed by SDS-PAGE, pooled, flash frozen, and stored at −80 °C for later use.

Sav1 GTPase and Nucleotide Exchange Assay.

Sav1 GTPase assays were carried out using a malachite green phosphate detection assay.[50] Then, 15 μg of Sav1 per reaction was preincubated with 50 μg/mL **1** or DMSO for 30 min at 30 °C in the assay buffer (10 mM Tris HCl, 10 mM NaCl, 2 mM $MgCl_2$ pH 7.4); then, the reaction was started with the addition of the assay buffer containing 100 μM GTP and incubated at 30 °C. At each time point, the reaction was stopped by the addition of 0.1 M EDTA (pH8) and then diluted 1:4 in water. Reactions were cooled to RT for 30 min before the addition of 20 μL of malachite green reagent (Sigma) and then incubated at RT in the dark for 35 min. Abs_{650} was measured, and the phosphate concentration was calculated based on a standard curve.

Nucleotide exchange assays were performed as previously described.[38,51] Recombinant Sav1 was incubated with a 20-fold molar excess of mantGDP (Sigma) and a 5-fold molar excess of EDTA over $MgCl_2$ for 1 h at RT. Reactions were stopped with the addition of 10 mM $MgCl_2$; then, the buffer was exchanged for 10 mM HEPES at pH 7.5, 50 mM NaCl, 2 mM $MgCl_2$, and 5 mM DTT using a NAP-5 column (GE Healthcare). Then, 5 μM mantGDP-loaded Sav1 was used in each reaction and preincubated with DMSO or 1 (30 μM) for 30 min. The exchange reaction was started with the addition of 5 μM GppNHp (Abcam), and Ex 360 Em 440 was measured every 33 s for 45 min using a SpectraMax i3x (Molecular Devices) plate reader. The reactions were performed in at least duplicates, and independent experiments were performed on different days.

Fluorescence Microscopy of Ds-Red-Labeled Sav1 in *C. neoformans*.

An overnight culture of DsRed-Sav1 was diluted to 1×10^6 cells/ml in YNB (Difco) with 2 μg/mL **1** or DMSO. Cells were incubated for 18 h at 37 °C and then imaged in bright field and red channels using a Nikon epifluorescence microscope with a Cool Snap HQ2 camera and Nikon Elements image acquisition and analysis software. The images were processed in Photoshop, only in order to increase the ease of viewing. All images were adjusted equally.

Sav1 Thermal Shift Assay.

Thermal shift assays were performed in 96-well plates on a CFX96 Touch real-time PCR system (Bio-Rad) using SYPRO Orange (Invitrogen). The final concentrations of Sav1 and SYPRO Orange used were 0.3 mg/mL and 4×, respectively. The reactions of 20 μL were carried out in triplicate in 50 mM HEPES at pH 8.0, 150 mM NaCl, 1 mM THP, 5% glycerol, and 3% DMSO using a temperature ramp from 25 to 95 °C. These data were fit using NAMI[52] to calculate the melting temperatures (T_M) values, which were used to assess the binding of ligands to Sav1.

Transmission Electron Microscopy.

An overnight H99 culture was diluted to 1×10^7 CFU/mL in 10% Sabauraud dextrose agar at pH 8 with 2 μg/mL **1** or DMSO. After 24 h of incubation at 37 °C, the cell pellets were collected and fixed with 2.5% glutaraldehyde (in 0.1 M sodium cacodylate buffer [pH 7.4]) overnight at 4 °C and then postfixed with 1% osmium tetroxide for 1 h. Following serial alcohol dehydration (50%, 75%, 95%, and 100%), the samples were embedded in Epon 12 (Ted Pella, Redding, CA). Ultramicrotomy was performed, and ultrathin sections (70 nm) were poststained with uranyl acetate and lead citrate. Samples were examined with a JEOL 1230 transmission electron microscope (TEM) (Tokyo, Japan).

Murine Model of Disseminated Cryptococcosis.

For escalating dose studies, CD-1 females (Envigo), 25–30 g were given 0, 10, 25, 50, or 100 mg/kg **1** *via* intraperitoneal (IP) injection once daily for 6 consecutive days ($n = 3$ mice per group). Then, **1** was formulated with 5% DMSO in 20% Kolliphor RH 40 in D5W. The mice were weighed daily and monitored for other symptoms of toxicity. For *in vivo* efficacy studies, C. *neoformans* H99 was cultured in 25 mL of YPD for 48 h, and then, the cells were washed three times with sterile PBS, enumerated with a hemocytometer, and diluted to 1.9 ×

10^6 CFU/mL in sterile PBS. CD-1 females (Envigo) (25–30 g) were inoculated with 3.8×10^5 CFUs (200 μL) by tail-vein injection. Starting 1 h postinoculation, the mice were given 50 mg/kg 1 or vehicle every 8 h for 48 h *via* IP injection ($n = 10$ per group). The brains were harvested 48 h postinoculation and homogenized in 1 mL of sterile PBS, and then, 10-fold dilutions were plated on YPD. Mice were housed 5 per cage and had access to food and water *ad libitum*.

Pharmacological Characterization of 1 in Mice.

Twenty-one female CD-1 mice were dosed *via* IP injection with 50 mg/kg 1 (Chem Bridge #7794378). Whole blood was collected in a syringe coated with anticoagulant citrate dextrose (ACD). Plasma was processed from whole blood by centrifugation at 10000 rpm for 10 min. Brain tissue was harvested and was gently washed with 1× PBS to remove residual circulating blood. The tissue was weighed and snap frozen in liquid nitrogen.

Plasma Processing.—For the standards and quality controls, 98 μL and 98.8 μL of blank vendor plasma was added to a microfuge tube and spiked with 2 and 1.2 μL of the initial standard. Standards, quality controls, and samples of 100 μL were then precipitated with 200 μL of methanol containing 0.15% formic acid and 12.5 ng/mL IS (final concentration). The samples were vortexed for 15 s, incubated at room temp for 10 min, and centrifuged at 13200 rpm twice in a standard microcentrifuge. The supernatant was then analyzed by LC-MS/MS. Vendor-supplied plasma used in the standards and quality controls (QCs) includes the following: Bioreclamation, LLC; lot #MSE284936; ACD anticoagulant.

Brain Processing.—Brain tissues were homogenized in 3X volume of PBS (X = weight of the tissue). For the standards and quality control samples, 98 μL and 98.8 μL of pooled blank brain was added to a microfuge tube and spiked with 2 or 1.2 μL of the initial standard. Standards and QC samples of 100 μL were then precipitated with 200 μL of methanol containing 0.15% formic acid and 12.5 ng/mL IS (final concentrations). The samples were vortexed for 15 s, incubated at room temp for 10 min, and centrifuged at 13200 rpm twice in a standard microcentrifuge. The supernatant was then analyzed by LC-MS/MS.

Ethics Statement.

The Guide for the Care and Use of Laboratory Animals of the National Research Council was strictly followed for all animal experiments. The animal experiment protocols were approved by Institutional Animal Care and Use Committees at the University of Iowa and the University of Texas Southwestern.

Supplementary Material

Refer to Web version on PubMed Central for supplementary material.

ACKNOWLEDGMENTS

The authors would like to thank John Perfect (Duke University), Robb Cramer (Dartmouth College), John Panepinto (University at Buffalo), Andy Alspaugh (Duke University), and Ping Wang (Louisiana State University)

for providing key strains and reagents as well as Tamara Doering (Washington University) for helpful discussions. This work was supported by a grant from the National Institute of Health 1R21AI125094 to D.J.K.

ABBREVIATIONS

BTU	benzothiourea
BBB	blood-brain-barrier
CFU	colony-forming units
MIC	minimum inhibitory concentration
TEM	transmission electron microscopy

REFERENCES

(1). Brown GD, Denning DW, Gow NAR, Levitz SM, Netea MG, and White TC (2012) Hidden Killers: Human Fungal Infections. Sci. Transl. Med 4 (165), 165rv13–165rv13.

(2). Rajasingham R, Smith RM, Park BJ, Jarvis JN, Govender NP, Chiller TM, Denning DW, Loyse A, and Boulware DR (2017) Global Burden of Disease of HIV-Associated Cryptococcal Meningitis: An Updated Analysis. Lancet Infect. Dis 17 (8), 873–881. [PubMed: 28483415]

(3). Bicanic T, Muzoora C, Brouwer AE, Meintjes G, Longley N, Taseera K, Rebe K, Loyse A, Jarvis J, Bekker L, Wood R, Limmathurotsakul D, Chierakul W, Stepniewska K, White NJ, Jaffar S, and Harrison TS (2009) Independent Association between Rate of Clearance of Infection and Clinical Outcome of HIV-Associated Cryptococcal Meningitis: Analysis of a Combined Cohort of 262 Patients. Clin. Infect. Dis 49 (5), 702–709. [PubMed: 19613840]

(4). Larsen RA, Leal MA, and Chan LS (1990) Fluconazole Compared with Amphotericin B plus Flucytosine for Cryptococcal Meningitis in AIDS. A Randomized Trial. Ann. Intern. Med 113 (3), 183–187. [PubMed: 2197908]

(5). Day JN, Chau TTHH, Wolbers M, Mai PP, Dung NT, Mai NH, Phu NH, Nghia HD, Phong ND, Thai CQ, Thai LH, Chuong LV, Sinh DX, Duong VA, Hoang TN, Diep PT, Campbell JI, Sieu TPMM, Baker SG, Chau NVVV, Hien TT, Lalloo DG, and Farrar JJ (2013) Combination Antifungal Therapy for Cryptococcal Meningitis. N. Engl. J. Med 368 (14), 1291–1302. [PubMed: 23550668]

(6). Hartland K, Pu J, Palmer M, Dandapani S, Moquist PN, Munoz B, DiDone L, Schreiber SL, and Krysan DJ (2016) High-Throughput Screen in *Cryptococcus neoformans* Identifies a Novel Molecular Scaffold That Inhibits Cell Wall Integrity Pathway Signaling. ACS Infect. Dis 2 (1), 93–102. [PubMed: 26807437]

(7). Gerik KJ, Donlin MJ, Soto CE, Banks AM, Banks IR, Maligie MA, Selitrennikoff CP, and Lodge JK (2005) Cell Wall Integrity Is Dependent on the PKC1 Signal Transduction Pathway in *Cryptococcus neoformans*. Mol. Microbiol 58 (2), 393–408. [PubMed: 16194228]

(8). Novick P, and Schekman R (1979) Secretion and Cell-Surface Growth Are Blocked in a Temperature-Sensitive Mutant of *Saccharomyces cerevisiae*. Proc. Natl. Acad. Sci. U. S. A 76 (4), 1858–1862. [PubMed: 377286]

(9). Novick P, Ferro S, and Schekman R (1981) Order of Events in the Yeast Secretory Pathway. Cell 25 (2), 461–469. [PubMed: 7026045]

(10). Novick P, Field C, and Schekman R (1980) Identification of 23 Complementation Groups Required for Post-Translational Events in the Yeast Secretory Pathway. Cell 21 (1), 205–215. [PubMed: 6996832]

(11). Feyder S, De Craene JO, Bar S, Bertazzi DL, and Friant S (2015) Membrane Trafficking in the Yeast *Saccharomyces cerevisiae* Model. Int. J. Mol. Sci 16 (1), 1509–1525. [PubMed: 25584613]

(12). Guo W, Roth D, Walch-Solimena C, and Novick P (1999) The Exocyst Is an Effector for Sec4P, Targeting Secretory Vesicles to Sites of Exocytosis. EMBO J. 18 (4), 1071–1080. [PubMed: 10022848]

(13). TerBush DR, Maurice T, Roth D, and Novick P (1996) The Exocyst Is a Multiprotein Complex Required for Exocytosis in *Saccharomyces cerevisiae*. EMBO J. 15 (23), 6483–6494. [PubMed: 8978675]

(14). Heider MR, Gu M, Duffy CM, Mirza AM, Marcotte LL, Walls AC, Farrall N, Hakhverdyan Z, Field MC, Rout MP, Frost A, and Munson M (2016) Subunit Connectivity, Assembly Determinants and Architecture of the Yeast Exocyst Complex. Nat. Struct. Mol. Biol 23 (1), 59–66. [PubMed: 26656853]

(15). Novick P, Brennwald P, Walworth NC, Kabcenell AK, Garrett M, Moya M, Roberts D, Müller H, Govindan B, and Bowser R (1993) in The Cycle of SEC4 Function in Vesicular Transport In Ciba Foundation Symposium 176–The GTPase Superfamily (Goode J, and Marsh J, Eds.) Vol. 176, pp 218–228, Ciba Foundation.

(16). Walworth NC, Brennwald P, Kabcenell AK, Garrett M, and Novick P (1992) Hydrolysis of GTP by Sec4 Protein Plays an Important Role in Vesicular Transport and Is Stimulated by a GTPase-Activating Protein in *Saccharomyces cerevisiae*. Mol. Cell. Biol 12 (5), 2017–2028. [PubMed: 1569938]

(17). Walworth NC, Goud B, Kabcenell AK, and Novick PJ (1989) Mutational Analysis of SEC4 Suggests a Cyclical Mechanism for the Regulation of Vesicular Traffic. EMBO J. 8 (6), 1685–1693. [PubMed: 2504585]

(18). Chayakulkeeree M, Johnston SA, Oei JB, Lev S, Williamson PR, Wilson CF, Zuo X, Leal AL, Vainstein MH, Meyer W, Sorrell TC, May RC, and Djordjevic JT (2011) SEC14 Is a Specific Requirement for Secretion of Phospholipase B1 and Pathogenicity of *Cryptococcus neoformans*. Mol. Microbiol 80 (4), 1088–1101. [PubMed: 21453402]

(19). Yoneda A, and Doering TL (2006) A Eukaryotic Capsular Polysaccharide Is Synthesized Intracellularly and Secreted via Exocytosis. Mol. Biol. Cell 17 (12), 5131–5140. [PubMed: 17021252]

(20). Panepinto J, Komperda K, Frases S, Park YD, Djordjevic JT, Casadevall A, and Williamson PR (2009) Sec6-Dependent Sorting of Fungal Extracellular Exosomes and Laccase of *Cryptococcus neoformans*. Mol. Microbiol 71 (5), 1165–1176. [PubMed: 19210702]

(21). Yoneda A, and Doering TL (2009) An Unusual Organelle in *Cryptococcus neoformans* Links Luminal pH and Capsule Biosynthesis. Fungal Genet. Biol 46 (9), 682–687. [PubMed: 19450701]

(22). Tucker SC, and Casadevall A (2002) Replication of *Cryptococcus neoformans* in Macrophages Is Accompanied by Phagosomal Permeabilization and Accumulation of Vesicles Containing Polysaccharide in the Cytoplasm. Proc. Natl. Acad. Sci. U. S. A 99 (5), 3165–3170. [PubMed: 11880650]

(23). Charlier C, Nielsen K, Daou S, Brigitte M, Chretien F, and Dromer F (2009) Evidence of a Role for Monocytes in Dissemination and Brain Invasion by *Cryptococcus neoformans*. Infect. Immun 77 (1), 120–127. [PubMed: 18936186]

(24). Herrmann JL, Dubois N, Fourgeaud M, Basset D, and Lagrange PH (1994) Synergic Inhibitory Activity of Amphotericin- b and γ Interferon against Intracellular *Cryptococcus neoformans* in Murine Macrophages. J. Antimicrob. Chemother 34 (6), 1051–1058. [PubMed: 7730221]

(25). O'Meara TR, and Alspaugh JA (2012) The Cryptococcus neoformans Capsule: A Sword and a Shield. Clin. Microbiol. Rev 25 (3), 387–408. [PubMed: 22763631]

(26). Williamson PR, Wakamatsu K, and Ito S (1998) Melanin Biosynthesis in *Cryptococcus neoformans*. J. Bacteriol 180 (6), 1570– 1572. [PubMed: 9515929]

(27). Williamson PR (1994) Biochemical and Molecular Characterization of the Diphenol Oxidase of *Cryptococcus neoformans*: Identification as a Laccase. J. Bacteriol 176 (3), 656–664. [PubMed: 8300520]

(28). Casadevall A, Rosas AL, and Nosanchuk JD (2000) Melanin and Virulence in *Cryptococcus neoformans*. Curr. Opin. Microbiol 3 (4), 354–358. [PubMed: 10972493]

(29). Zhu X, Gibbons J, Garcia-Rivera J, Casadevall A, and Williamson PR (2001) Laccase of *Cryptococcus neoformans* Is a Cell Wall-Associated Virulence Factor. Infect. Immun 69 (9), 5589–5596. [PubMed: 11500433]

(30). Missall TA, Moran JM, Corbett JA, and Lodge JK (2005) Distinct Stress Responses of Two Functional Laccases in *Cryptococcus neoformans* Are Revealed in the Absence of the Thiol-Specific Antioxidant Tsa1. Eukaryotic Cell 4 (1), 202–208. [PubMed: 15643075]

(31). Sabiiti W, Robertson E, Beale MA, Johnston SA, Brouwer AE, Loyse A, Jarvis JN, Gilbert AS, Fisher MC, Harrison TS, May RC, and Bicanic T (2014) Efficient Phagocytosis and Laccase Activity Affect the Outcome of HIV-Associated Cryptococcosis. J. Clin. Invest 124 (5), 2000–2008. [PubMed: 24743149]

(32). Van Rijn HJ, Boer P, and Steyn-Parvé EP (1972) Biosynthesis of Acid Phosphatase of Baker's Yeast. Factors Influencing Its Production by Protoplasts and Characterization of the Secreted Enzyme. Biochim. Biophys. Acta - Enzymol 268 (2), 431–441.

(33). Levin DE (2011) Regulation of Cell Wall Biogenesis in *Saccharomyces cerevisiae*: The Cell Wall Integrity Signaling Pathway. Genetics 189 (4), 1145–1175. [PubMed: 22174182]

(34). Abe M, Qadota H, Hirata A, and Ohya Y (2003) Lack of GTP-Bound Rho1p in Secretory Vesicles of *Saccharomyces cerevisiae*. J. Cell Biol 162 (1), 85–97. [PubMed: 12847085]

(35). Powers-Fletcher MV, Feng X, Krishnan K, and Askew DS (2013) Deletion of the Sec4 Homolog SrgA from Aspergillus fumigatus Is Associated with an Impaired Stress Response, Attenuated Virulence and Phenotypic Heterogeneity. PLoS One 8 (6), No. e66741. [PubMed: 23785510]

(36). Sudan A, Livermore J, Howard SJ, Al-Nakeeb Z, Sharp A, Goodwin J, Gregson L, Warn PA, Felton TW, Perfect JR, Harrison TS, and Hope WW (2013) Pharmacokinetics and Pharmacodynamics of Fluconazole for Cryptococcal Meningoencephalitis: Implications for Antifungal Therapy and in Vitro Susceptibility Breakpoints. Antimicrob. Agents Chemother 57 (6), 2793–2800. [PubMed: 23571544]

(37). Müller MP, and Goody RS (2018) Molecular Control of Rab Activity by GEFs. GAPs and GDI. Small GTPases 9 (1–2), 5–21. [PubMed: 28055292]

(38). Itzen A, Rak A, and Goody RS (2007) Sec2 Is a Highly Efficient Exchange Factor for the Rab Protein Sec4. J. Mol. Biol 365 (5), 1359–1367. [PubMed: 17134721]

(39). Gao X, Albert S, Tcheperegine SE, Burd CG, Gallwitz D, and Bi E (2003) The GAP Activity of Msb3p and Msb4p for the Rab GTPase Sec4p Is Required for Efficient Exocytosis and Actin Organization. J. Cell Biol 162 (4), 635–646. [PubMed: 12913108]

(40). Dai R, Wilson DJ, Geders TW, Aldrich CC, and Finzel BC (2014) Inhibition of *Mycobacterium tuberculosis* Transaminase BioA by Aryl Hydrazines and Hydrazides. ChemBioChem 15 (4), 575–586. [PubMed: 24482078]

(41). Levitz SM, and DiBenedetto DJ (1989) Paradoxical Role of Capsule in Murine Bronchoalveolar Macrophage-Mediated Killing of *Cryptococcus neoformans*. J. Immunol 142 (2), 659–665. [PubMed: 2521352]

(42). Bolaños B, and Mitchell TG (1989) Phagocytosis of *Cryptococcus neoformans* by Rat Alveolar Macrophages. Med. Mycol 27 (4), 203–217.

(43). Wang Y, Aisen P, and Casadevall A (1995) *Cryptococcus neoformans* Melanin and Virulence: Mechanism of Action. Infect. Immun 63 (8), 3131–3136. [PubMed: 7622240]

(44). Wang Y, and Casadevall A (1994) Growth of *Cryptococcus neoformans* in Presence of L-Dopa Decreases Its Susceptibility to Amphotericin B. Antimicrob. Agents Chemother 38 (11), 2648–2650. [PubMed: 7872761]

(45). Andes DR, and Lepak AJ (2011) Antifungal Pharmacokinetics and Pharmacodynamics Essentials Clin. Mycol Second Ed., 121–134.

(46). Pardridge WM (2005) The Blood-Brain Barrier: Bottleneck in Brain Drug Development. NeuroRx 2 (1), 3–14. [PubMed: 15717053]

(47). CLSI (2017) in Reference Method for Broth Dilution Antifungal Susceptablity Testing of Filamentous Fungi 3rd ed., Clinical and Labratory Standards Institute, Wayne, PA.

(48). CLSI (2017) in Reference Method for Broth Dilution Antifungal Susceptibility Testing of Yeasts 4th ed., Clinical and Labratory Standards Institute, Wayne, PA.

(49). Meletiadis J, Pournaras S, Roilides E, and Walsh TJ (2010) Defining Fractional Inhibitory Concentration Index Cutoffs for Additive Interactions Based on Self-Drug Additive Combinations, Monte Carlo Simulation Analysis, and *in vitro-in vivo* Correlation Data for

Antifungal Drug Combinations against *Aspergillus fumigatus*. Antimicrob. Agents Chemother 54 (2), 602–609. [PubMed: 19995928]

(50). Leonard M, Doo Song B, Ramachandran R, and Schmid SL (2005) Robust Colorimetric Assays for Dynamin's Basal and Stimulated GTPase Activities. Methods in Enzymology 404, 490–503. [PubMed: 16413294]

(51). Kanie T, and Jackson P (2018) Guanine Nucleotide Exchange Assay Using Fluorescent MANT-GDP. BIO-PROTOCOL 8 (7), 1.

(52). Grøftehauge MK, Hajizadeh NR, Swann MJ, and Pohl E (2015) Protein-Ligand Interactions Investigated by Thermal Shift Assays (TSA) and Dual Polarization Interferometry (DPI). Acta Crystallogr., Sect. D: Biol. Crystallogr 71 (1), 36–44. [PubMed: 25615858]

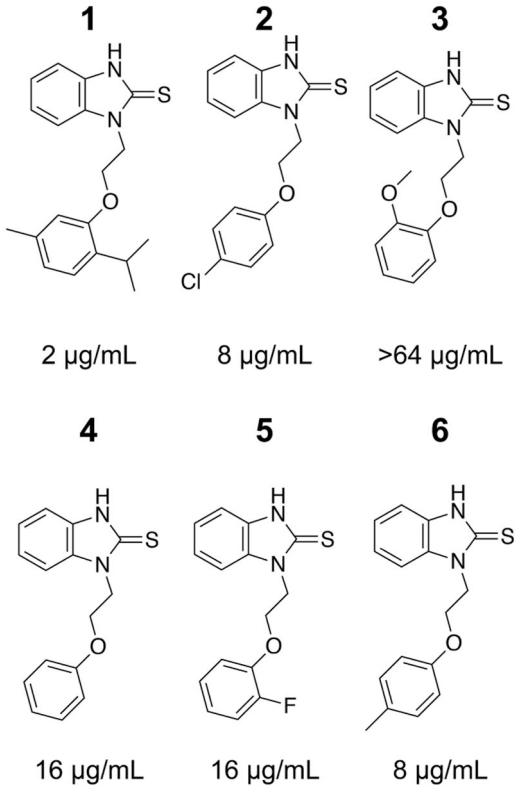

Figure 1.

Structure-activity relationship of BTU derivatives. Each benzothiourea compound is shown with the minimum inhibitory concentration (MIC) against *C. neoformans* H99. MIC values are representative from at least two independent assays using standard CLSI methods.

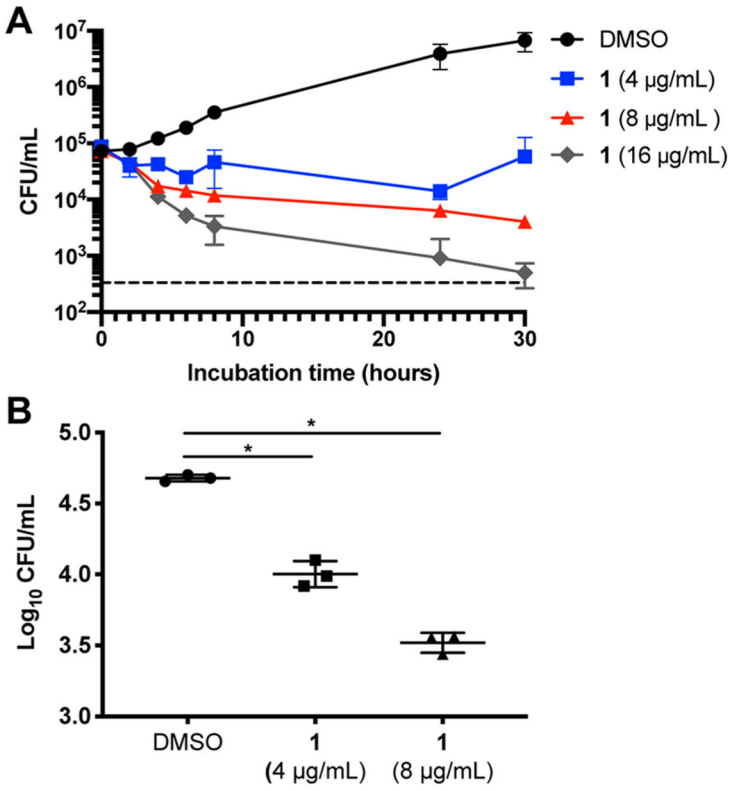

Figure 2.

BTU derivatives are fungicidal and active against intracellular *C. neoformans*. (A) Time kill assays show **1** is fungicidal at 8 and 16 μg/mL over 30 h. Data represent the mean and SD of triplicates and are representative of two independent experiments. The dashed line denotes the limit of detection. (B) Colony forming units (CFUs) of intracellular *C. neoformans*, phagocytosed by J774 cells and treated with compound **1** for 24 h, are significantly reduced. Data represent the mean and SD of triplicates and are representative of two independent experiments. *$p < 0.0002$ by unpaired *t* test compared to control.

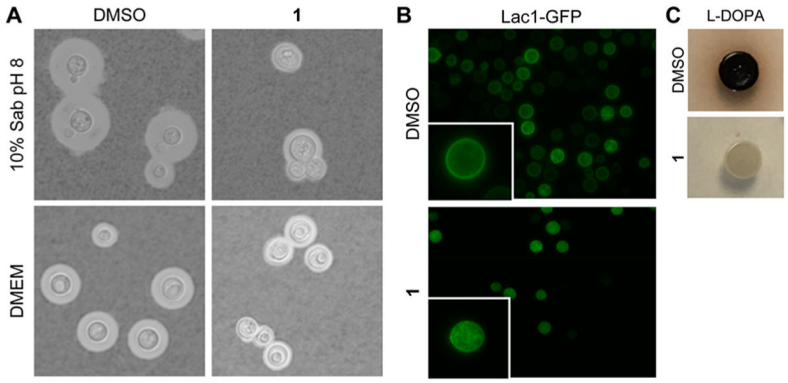

Figure 3.

Expression of *C. neoformans* virulence factors is inhibited by BTU derivatives. (A) India ink staining of cells grown in 10% Sab pH 8 or DMEM shows **1** (2ug/mL) reduces capsule size after 24 (Sab) or 48 (DMEM) hours. (B) Lac1-GFP is mislocalized from the cell periphery to the cytoplasm when treated with **1** (2 μg/mL). (C) **1** (8 μg/mL) inhibits melanization on solid media containing L-DOPA. Images taken after 3 days of growth. All images are representative of at least two independent experiments.

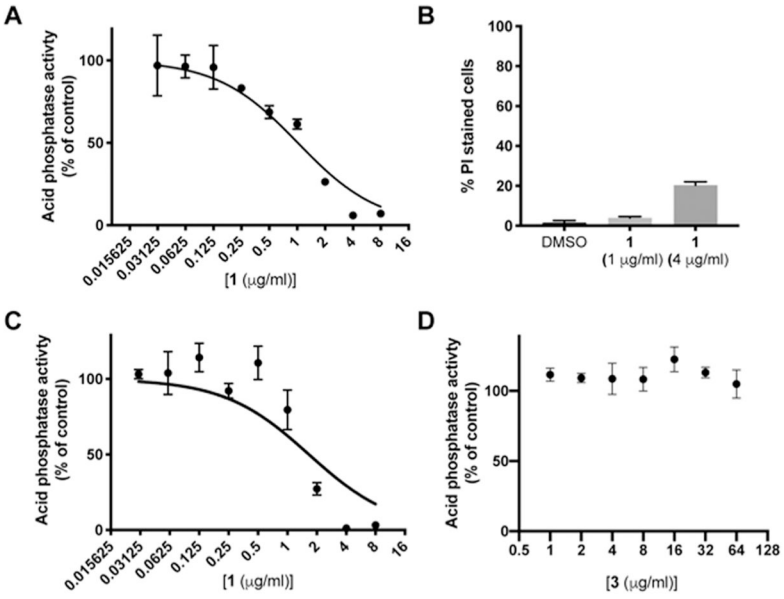

Figure 4.

Acid phosphatase secretion is inhibited by BTU compounds. (A) IC_{50} curve of cell-associated acid phosphatase activity after 6 h of treatment with **1**. (B) Percentage of cells that stain positive with propidium iodide (PI) after 6 h of exposure to indicated concentrations of **1**. Data represent mean and SD of triplicates with at least 100 cells counted per replicate. (C and D) IC50 curves of (C) **1** and (D) **3** after 18 h of treatment. (A, C, and D) Data are plotted as mean and SD of triplicates expressed as percent of DMSO control and are representative of two independent experiments.

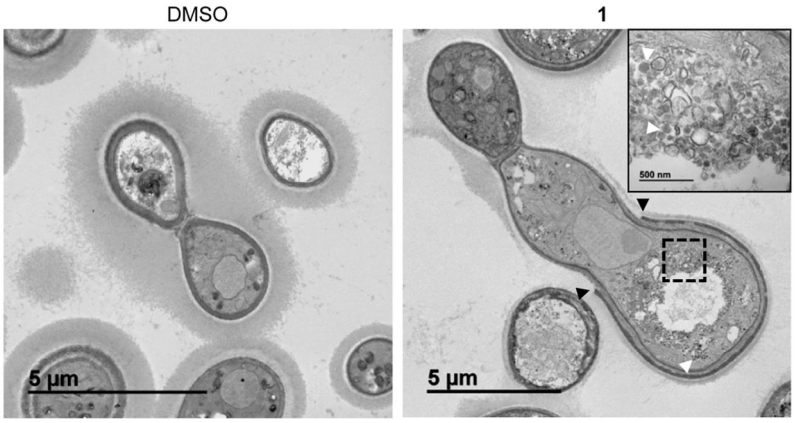

Figure 5.

BTU derivatives induce cell-wall defects and accumulation of intracellular vesicles. TEM images of cells grown in 10% Sab pH 8 for 24 h. Treatment with **1** (2 μg/mL) results in an incomplete cell wall (black arrows) around the cell body and the accumulation of vesicles within the cell (white arrows). Inset shows magnification of boxed area.

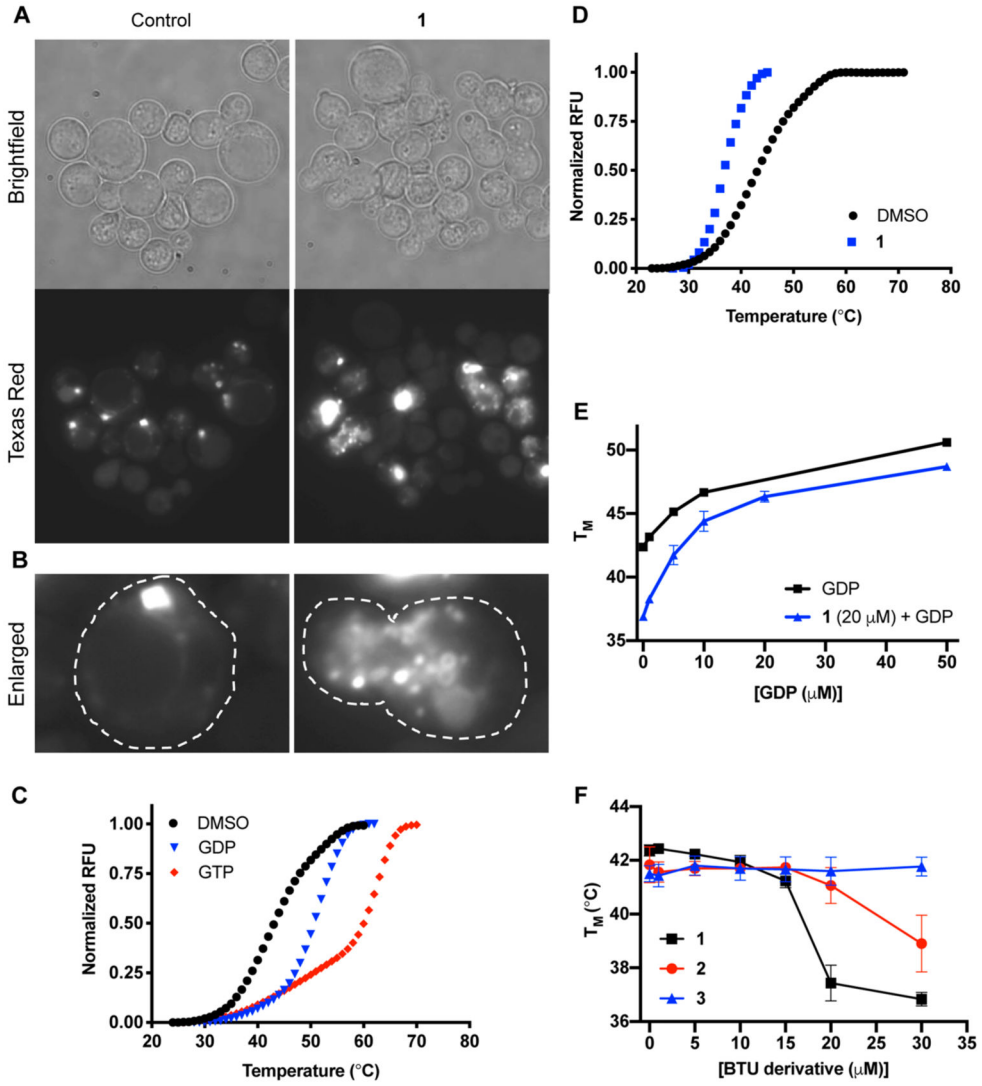

Figure 6.

BTU derivatives interact with the small GTPase Sav1. (A) Images of DsRed-Sav1 treated with DMSO or **1** (2 μg/mL). (B) Enlarged frame shows a single cell from each representative image with the cell perimeter outlined in white dashed lines. Images taken at 100×. (C and D) Thermal-shift curves of recombinant Sav1 with 50 μM GTP or GDP show binding to both ligands. (D) With the addition of **1** (20 μM) the stability of Sav1 decreases. Representative reactions of triplicates. (E and F) Melting temperatures (T_M) of Sav1, as determined by the thermal shift, with increasing concentrations of GDP with or without (F; 30 μM) **1** or (E) **1**, **2** and **3** or with increasing concentrations. Data represent mean and SD of triplicates.

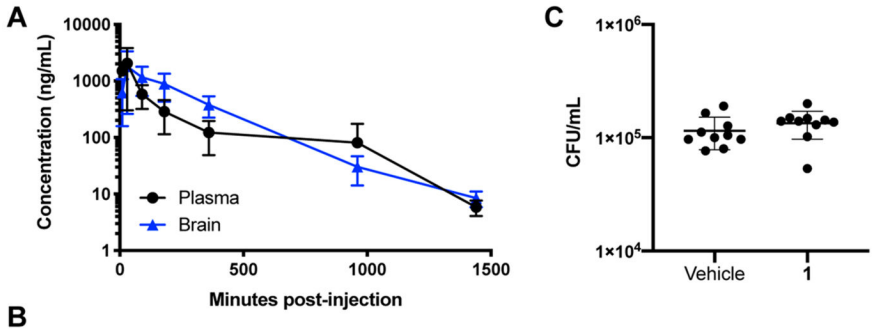

B

Parameter	Unit	Plasma Estimate	Brain Estimate
$T_{1/2}$	min	239.48	183.93
T_{max}	min	30	30
C_{max}	ng/mL	2055.13	1801.81
AUC	min*ng/mL	279758.33	455145.87

Figure 7.

Pharmacokinetics of BTU derivatives are favorable and penetrate the blood brain barrier. (A) *In vivo* pharmacokinetics of **1** given as a single 50 mg/kg dose. Data represent mean and SD of 3 mice per group. (B) Values for the half-life ($T_{1/2}$), maximum concentration (C_{max}), time of maximum concentration (T_{max}), and area under the curve (AUC). (C) CFU counts from brains of mice treated every 8 h for 48 h with vehicle or **1** (50 mg/kg). n = 10 mice/group. Data are plotted as individual data points with mean and SD.

Table 1.

Minimum Inhibitory Concentrations of Compound 1 against Yeast and Mold Species[a]

species	strain	MIC (μg/mL)
C. *neoformans*	H99	2
	JEC21	4
	DUMC 138.99	2
	DUMC 158.03	4
	DUMC 153.02	4
	DUMC 266.03	4
	DUMC 101.14	4
	DUMC 120.04	4
	DUMC 118.00	4
	DUMC 111.00	2
S. cerevisiae	BY4741	>128
C. albicans	SC5314	>64
A. fumigatus	AF293	>64
	CEA10	>64
Fusarium solani	DUMC 132.02	>64
F. oxysporum	DUMC 124.02	>64
M. circinelloides	CBS277.49	4–8

[a]Minimum inhibitory concentrations (MIC) as determined by CLSI methods. Data are from at least two independent experiments performed on different days.